



Sensitivity analysis of the geomorphology flood index to extreme rainfall variability in Indonesia

Jessica Amanda Bintang^{1,*}

¹ Study Program of Meteorology, Faculty of Earth Sciences and Technology, Institut Teknologi Bandung, Bandung, West Java 40132, Indonesia.

*Correspondence: Jessicaamnd@gmail.com

Received Date: June 1, 2024

Revised Date: July 20, 2024

Accepted Date: July 31, 2024

ABSTRACT

Background: Flooding is one of the most frequent and costly natural disasters worldwide. According to DIBI-BNPB data, Indonesia has experienced 11,806 flood events. Flood risk management is crucial to identify flood-prone areas, which can be done through Flood Hazard Mapping (FHM) using the Geomorphology Flood Index (GFI). While GFI relies on topographical factors, Indonesia's rainfall varies significantly, necessitating a sensitivity comparison across different extreme rainfall characteristics. **Methods:** This study compares conventional GFI (without rainfall) and modified GFI (incorporating extreme rainfall). It determines extreme rainfall return periods of 5, 10, 25, 50, and 100 years using the Generalized Extreme Value (GEV) method. These values are normalized into Ip-A and Ip-B indices, which are then integrated into the GFI model to estimate flood-prone areas. **Findings:** The Ip-A and Ip-B methods yield different results. At a 100-year return period, Ip-A produces the same flood extent as conventional GFI, whereas Ip-B varies. Maluku, with the highest extreme rainfall (323.91 mm/day), shows a larger flood extent than conventional GFI, while Java, with the lowest (188.11 mm/day), shows a smaller extent. Extreme rainfall variability significantly affects flood potential, making the Ip-B method highly sensitive to such variations. **Conclusion:** The study concludes that the Ip-A method produces flood potential areas similar to the conventional GFI at a 100-year return period, while the Ip-B method yields different flood extents depending on extreme rainfall intensity. The Ip-B method is highly sensitive to extreme rainfall variations, making it more responsive to regional differences in flood potential. **Novelty/Originality of this article:** This study introduces a novel approach by integrating extreme rainfall variability into the Geomorphology Flood Index (GFI) using two modified indices, Ip-A and Ip-B, to enhance flood hazard mapping accuracy.

KEYWORDS: extreme rainfall; flood; flood hazard mapping; geomorphology flood index.

1. Introduction

Flood disasters are among the most frequent natural disasters worldwide and incur the highest costs compared to other disasters, as flood-related damages account for one-third of the economic losses caused by natural disasters. Therefore, flood risk management is essential to identify flood-prone areas within a region, which can be achieved through Flood Hazard Mapping (FHM) (Mudashiru et al., 2021). The flood hazard mapping method is categorized into three approaches: physically-based, physical modeling methods, and empirical (Bellos, 2012; Teng et al., 2017).

The physically-based and physical modeling methods provide more accurate results than the empirical approach; however, these methods require extensive resources and data, making them inefficient for large-scale areas. Over the past one to two decades, the

Cite This Article:

Bintang, J. A. (2024). Sensitivity analysis of the geomorphology flood index to extreme rainfall variability in Indonesia. *Calamity: A Journal of Disaster Technology and Engineering*, 2(1), 1-15. <https://doi.org/10.61511/calamity.v2i1.2024.1834>

Copyright: © 2024 by the authors. This article is distributed under the terms and conditions of the Creative Commons Attribution (CC BY) license (<https://creativecommons.org/licenses/by/4.0/>).



empirical method has been widely used by researchers as it enables broader regional assessments with minimal data and resource requirements. Although this method is less accurate, it remains highly efficient for large-scale flood hazard analysis.

One of the empirical approaches is the Geomorphology Flood Index (GFI). The GFI method is an effective tool for estimating flood inundation areas, particularly in large watershed regions with limited hydrological data (Samela et al., 2018). In Indonesia, GFI has been implemented in the technical module for flood disaster risk assessment developed by the National Disaster Management Agency (BNPB). The GFI approach utilizes two key components in its formula: H and hr , where H represents the elevation difference between the river and the watershed, while hr denotes the water depth at varying elevations (Samela, 2017).

Manfreda (2015) utilized hr to calculate the area (A_r) in square meters (m^2) from the tested point to the nearest river basin. However, this approach does not perform well in large areas with high rainfall variability. Therefore, a possible improvement is to convert the area (A_r) into rainfall volume (V_r) to better assess its sensitivity. The intensity of heavy rainfall is a crucial factor as it influences the scale of flood potential (Boers et al., 2016).

Kubro (2021) successfully incorporated rainfall data into the Geomorphology Flood Index (GFI) by transforming area (A_r) into volume (V_r). However, the resulting sensitivity was suboptimal due to similar rainfall characteristics and return periods, as well as the relatively small study areas of the Ciliwung and Citarum River Basins. This limitation may have arisen from errors in incorporating rainfall parameters or the uniformity of rainfall characteristics in the studied regions. Therefore, sensitivity testing using the Geomorphology Flood Index (GFI) method is required in a broader study area, covering all watersheds in Indonesia, to capture greater variability. This approach aims to thoroughly assess GFI sensitivity based on the recommendations of Kubro (2021).

Flooding is influenced by several factors, including elevation, topography, and rainfall. The Geomorphology Flood Index (GFI) method considers only topographical aspects, whereas rainfall exhibits significant variability. If the GFI method produces accurate results, it suggests that rainfall in the region is homogeneous, allowing it to be treated as a constant rather than a variable. However, in reality, rainfall varies considerably. A study by Kubro (2021) found that the modified GFI method yielded results similar to those of the conventional GFI. Sensitivity comparisons in adjacent areas showed no significant differences due to minimal rainfall variation. Therefore, a broader sensitivity comparison across regions with diverse rainfall characteristics is necessary to ensure the applicability of the GFI method in Indonesia.

1.1 Geomorphology flood index (GFI)

The Geomorphology Flood Index (GFI) is an effective method for estimating flood inundation areas, particularly in large-scale watersheds with limited hydrological data (Samela et al., 2018). The GFI method has been adopted in Indonesia within the technical module for flood disaster risk assessment, developed by BNPB (National Disaster Management Agency). Manfreda (2015) evaluated various flood indices and identified GFI as the most effective approach. This index compares water depth at different elevations (hr) with the elevation difference between the river and the watershed (H) (Samela, 2017).

Manfreda et al. (2015) used hr to calculate the area (A_r) in square meters (m^2) from the tested point to the nearest river basin. Therefore, hr is employed to account for water surface elevation in the adjacent drainage network as a flood hazard indicator. The GFI calculation formula is as follows:

$$GFI = \ln \frac{hr}{H} \text{ With } hr \approx bAr^n \quad (\text{Eq. 1})$$

The variables in the Geomorphology Flood Index (GFI) formula are defined as follows, hr refers to the water depth at different elevations, while H represents the elevation

difference between the tested element and the watershed. Additionally, A_r denotes the area of the river connected to the tested location, whereas n is the exponent calibrated based on the study area, and b is the scaling factor determined by the DEM used.

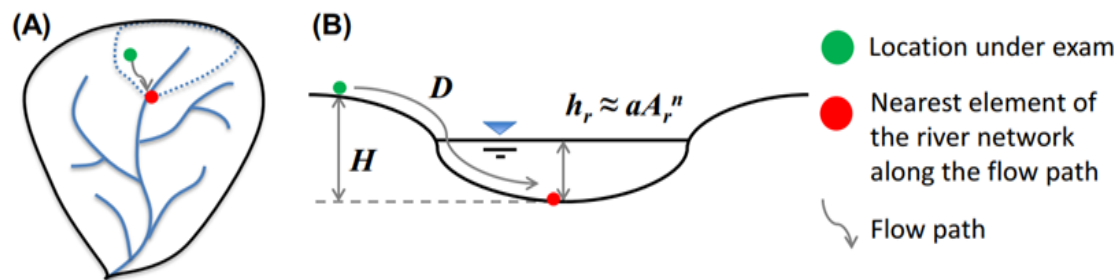


Fig. 1. Illustration of the GFI equation used to determine the flood hazard index (Samela et al., 2017)

1.2 GFI method experiment

In Figure 2, Manfreda & Samela (2019) conducted a study on the Geomorphology Flood Index (GFI) in the Bradano River, one of the major rivers in the Basilicata region of Southern Italy. Figure (a) illustrates the water depth at different elevations, Figure (b) depicts the elevation difference between the tested element and the watershed, and Figure (c) presents the GFI mapping results using the formula mentioned above. The GFI mapping results indicate that as h_r increases, the GFI index also increases. Conversely, if h_r is smaller than H , the GFI index decreases.

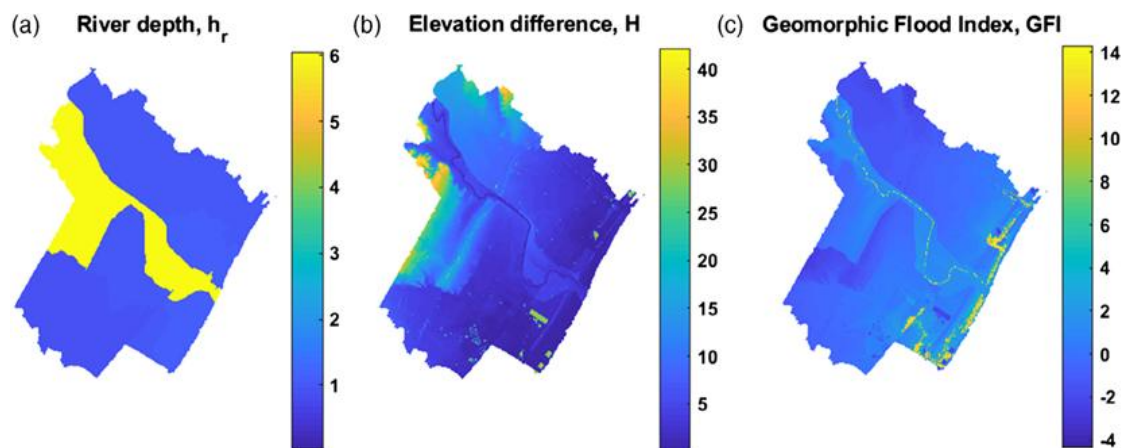


Fig. 2. GFI calculation process using DEM data (Manfreda et al., 2015)

The following figure presents GFI experiments conducted both internationally and domestically. Currently, there is no GFI map available for the entire Indonesia. Figure 3 presents three maps illustrating flood risk across the continental United States, based on data from two primary sources: FEMA (Federal Emergency Management Agency) and GFI (Global Flood Initiative). The first map shows the division of the U.S. into major drainage basins or hydrologic regions, labeled from 1 to 18. These regions represent the flow direction of water bodies and serve as the foundational geographic units for analyzing flood potential. The second map, provided by FEMA, displays flood zones based on historical data and hydrological assessments. Areas marked in yellow represent regions with a 1% annual chance of flooding—commonly referred to as the 100-year floodplain—while orange indicates areas with a 0.2% annual chance of flooding, or the 500-year floodplain. However, a significant portion of the country, particularly in the western regions, remains unclassified or unstudied by FEMA, as indicated by dark green shading.

The third map utilizes data from the GFI and offers a broader and more detailed view of flood-prone areas. Dark blue areas highlight regions at risk of 100-year floods, whereas light blue represents zones considered not prone to flooding according to GFI's global flood modeling approach. Compared to FEMA's map, the GFI data appears more comprehensive, especially in identifying flood risks in the western and southern parts of the United States—areas that FEMA has not thoroughly mapped. The contrast between FEMA and GFI maps underscores differences in methodologies used to assess flood hazards, which ultimately lead to varying delineations of flood-prone zones. These differences are crucial for policymaking, spatial planning, and disaster mitigation strategies, as discrepancies in data can significantly influence decisions related to infrastructure development, residential zoning, and public safety in the face of flood risks.

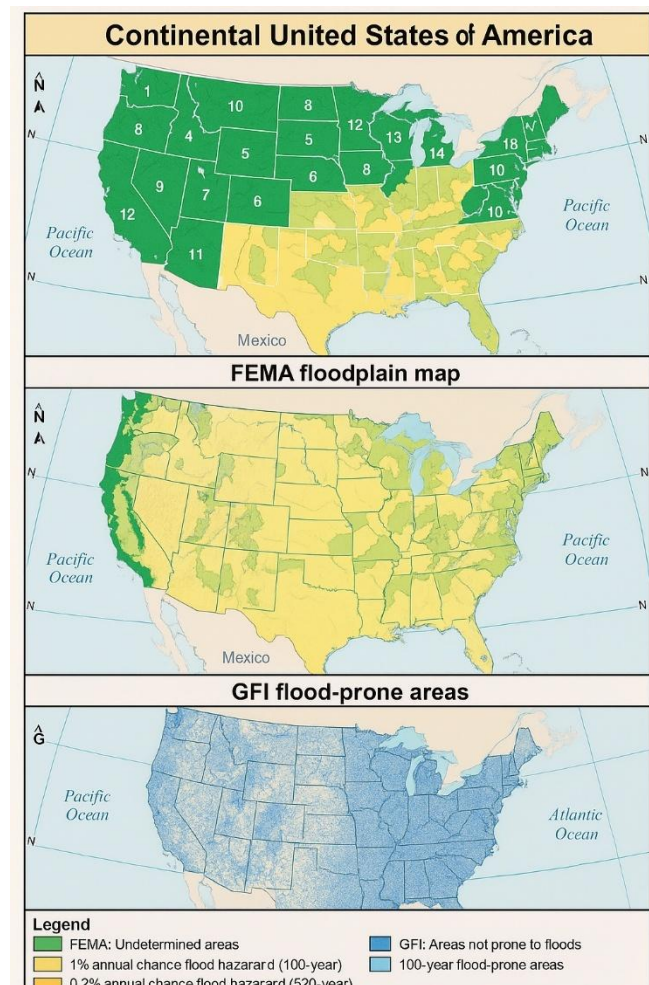


Fig. 3. GFI mapping in Americas
(Samela et al., 2017)

1.3 Generalized extreme value (GEV)

In probability and statistics theory, the Generalized Extreme Value (GEV) distribution describes the frequency distribution of the smallest and largest data values within a sample. This distribution was introduced by Fisher & Tippet (1928). The parameters in the Generalized Extreme Value (GEV) distribution are defined as follows: μ is the location parameter, where $-\infty < \mu < \infty$, and σ is the scale parameter, where $\sigma > 0$, while ξ represents the shape parameter. The GEV distribution used in this study is Type I GEV, also known as the Gumbel distribution. The Type I GEV or Gumbel distribution is defined when the ξ value is equal to 0. Furthermore, the Gumbel distribution is combined with the return period,

allowing the estimation of extreme rainfall values for specific return periods. In the GEV distribution, there is a random variable X , where this variable has the Cumulative Distribution Function (CDF) as follows:

$$f(x, \mu, \sigma, \xi) = \begin{cases} \exp \left\{ - \left(1 + \xi \left(\frac{x - \mu}{\sigma} \right) \right)^{-\frac{1}{\xi}} \right\}, & -\infty < x < \infty \neq 0, 1 + \xi \left(\frac{x - \mu}{\sigma} \right) > 0 \\ \exp \left\{ - \exp \left(- \frac{x - \mu}{\sigma} \right) \right\}, & -\infty < x < \infty, \xi = 0 \end{cases} \quad (\text{Eq. 2})$$

1.4 Extreme rainfall in Indonesia

According to Regulation of the Head of the Meteorology, Climatology, and Geophysics Agency (BMKG) No. KEP. 009 of 2010 on Standard Operating Procedures for Early Warning, Reporting, and Dissemination of Extreme Weather Information, extreme rainfall refers to heavy rain and hail. Heavy rain is defined as rainfall with a minimum intensity of 50 millimeters (mm) per 24 hours or 20 millimeters (mm) per hour (Parker & Gallant, 2022; Qiao et al., 2021).

1.5 Bankfull discharge

Bankfull discharge refers to a channel filled to its capacity without causing flooding. (Barrocu & Eslamian, 2022; Ghafuri et al., 2024; Sarker, 2023). Fluvial geomorphologists are particularly interested in bankfull discharge, as it can be applied in river engineering and restoration to design stable river dimensions and shapes, ensuring that the channel maintains its structure and pattern over time (Rosgen, 1994).

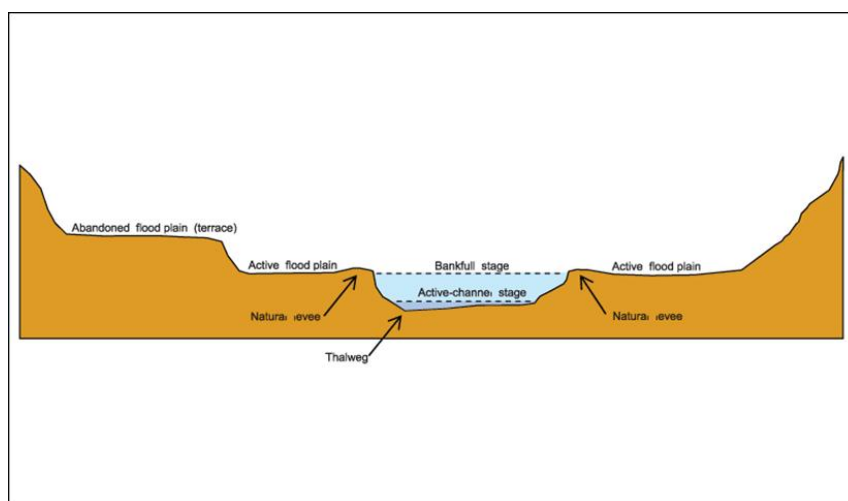


Fig. 5. Bankfull discharge when it reaches maximum point (Sherwood & Huitger, 2005)

Several researchers have investigated bankfull discharge in relation to return periods, ranging from 1–2 years, 4–10 years, and less than 2 years. However, determining bankfull discharge is highly complex and depends on the specific stream classification and conditions (Bastola & Diplas, 2023; Shojinaga et al., 2025; Zarrabi et al., 2025).

2. Methods

The data used in this study are as follows: the Digital Elevation Model (DEM) data, which comes from DEMNAS and represents all watersheds in Indonesia with a 1 km resolution and a World Mercator projection. Additionally, the rainfall data used in this study

is derived from the Global Precipitation Measurement (GPM) Level 3, specifically the GPM-IMERG Final Run Version 06B, with a spatial resolution of $0.1^\circ \times 0.1^\circ$ and a temporal resolution of 30 minutes for the period 2000–2021, and this data can be accessed at (<https://gpm.nasa.gov/data/directory/>). Furthermore, the river data for all of Indonesia used in this study originates from (<https://tanahair.indonesia.go.id/demnas/#/>), where the spatial resolution includes vector data (Indonesia base map) at a scale of 1:250,000.

Sensitivity testing of the GFI was conducted through a series of studies, and while conventional GFI processing uses only DEM data, modified GFI processing requires rainfall data. The modified GFI processing begins by analyzing climatological rainfall data across Indonesia to obtain the maximum rainfall, and once the maximum rainfall data is obtained, it is used to calculate the return periods for 5, 10, 25, 50, and 100 years. Subsequently, the data is incorporated into the modified GFI calculations by integrating DEM data using return periods of 10, 25, 50, and 100 years with Ip-A and Ip-B. Finally, sensitivity testing is performed, which results in flood hazard mapping using GFI Ip-A and GFI Ip-B, along with the corresponding area extents in each region with different extreme rainfall conditions.

There are two methods used in the GFI processing. First, the conventional GFI method utilizes only Digital Elevation Model (DEM) data, and second, the modified GFI method employs both DEM data and extreme rainfall data as additional parameters, since the study area is extensive and exhibits significant rainfall variability.

2.1 Extreme rainfall treatment

First, in probability and statistics theory, the Generalized Extreme Value (GEV) distribution describes the frequency distribution of the smallest and largest data values within a sample. This distribution was introduced by Fisher & Tippet (1928). The GEV type used in this study is Type I GEV, also known as the Gumbel Distribution. The Type I GEV or Gumbel Distribution is defined when the ξ value is equal to 0. Furthermore, the Gumbel Distribution is combined with the return period, allowing the estimation of extreme rainfall values for specific return periods.

Additionally, the return period represents the average interval of time between occurrences of an event at a specific magnitude or greater (Haan, 1977). In this study, extreme rainfall values are determined for two return periods: 5 years and 100 years, with a 24-hour duration. This process is conducted using Python programming with Global Precipitation Measurement (GPM) data in a grid format, ensuring that extreme rainfall values for each return period are calculated on a per-grid basis. Once the extreme rainfall values for each return period are obtained for each river region, they are incorporated as weights in the flow accumulation process, serving as input for the modified GFI calculation.

2.2 Conventional GFI calculation

The conventional GFI calculation is performed using the Geomorphology Flood Area plugin available in QGIS version 2.14.9. To obtain the GFI value, a constant threshold is required; however, a well-calibrated map of the study area is essential. Due to data limitations, the calibration process is conducted manually. The required data for GFI computation includes DEM, fill, flow direction, and flow accumulation. The GFI calculation is performed using ArcGIS version 10.3, and the results include the variables H, hr, and GFI.

2.3 Calculation of modified GFI

The modified GFI calculation incorporates extreme rainfall parameters by transforming Ar into Vr using the following equation:

$$hr = b(Vr)^n \quad (\text{Eq. 3})$$

The hr variable is derived from flow accumulation, where the calculation process includes the normalized return period of rainfall. The flow accumulation for each return period is used as an input in the modified GFI calculation. The application used for modified GFI calculation is the same as that used for conventional GFI calculation, with the key difference being the transformation of Ar into Vr using the rainfall return period. There are two methods for precipitation index calculation, namely $Ip-A$ and $Ip-B$, with the following equations:

$$Ip - A = \frac{Px - P5}{P100 - P5} \quad (\text{Eq. 4})$$

The variables in the precipitation index calculation are defined as follows: $Ip-A$ refers to the Precipitation Index A, while Px represents the return periods of 5, 10, 25, 50, and 100 years. Additionally, $P5$ is the lower threshold of the return period, indicating non-flood conditions, and $P100$ is the upper threshold of the return period, corresponding to flood conditions, which is the same as in the conventional GFI method.

$$Ip - B = \frac{Px - P5}{P100mean - P5} \quad (\text{Eq. 5})$$

The variables in the precipitation index calculation are defined as follows: $Ip-B$ refers to the Precipitation Index B, while Px represents the return periods of 5, 10, 25, 50, and 100 years. Additionally, $P5$ is the lower threshold of the return period, indicating non-flood conditions, and $P100mean$ is the average rainfall at the 100-year return period.

2.4 Sensitivity test

Sensitivity testing is conducted by comparing the GFI method with $Ip-A$ and $Ip-B$. Subsequently, this comparison is represented in a graph showing the increase or decrease in flood-prone areas using the following formula:

$$\text{Extent of Change} = \frac{\text{flood potential area of GFI } Ip-B - \text{flood potential area of GFI } Ip-A}{\text{Flood potential area of GFI } Ip-B} \quad (\text{Eq. 6})$$

3. Results and Discussion

3.1 Rainfall return period

In this study, rainfall values for each return period were estimated using the Gumbel distribution. The annual maximum data derived from GPM IMERG satellite data over a 20-year period was used to estimate extreme rainfall for return periods of 5, 10, 25, 50, and 100 years. Figure 6 presents the rainfall return periods of 10 and 100 years.

In Figure 6, it can be observed that rainfall for the 5-year return period has the smallest values compared to other return periods, with a minimum value of 58 mm/day and a maximum value of 331 mm/day. Meanwhile, the 100-year return period has a minimum value of 86 mm/day and a maximum value of 538 mm/day. The blue color scale represents the minimum values, while the red color scale represents the maximum values. Additionally, the rainfall patterns for each return period exhibit a consistent spatial distribution, indicating that the spatial variability of extreme rainfall remains constant across return periods.

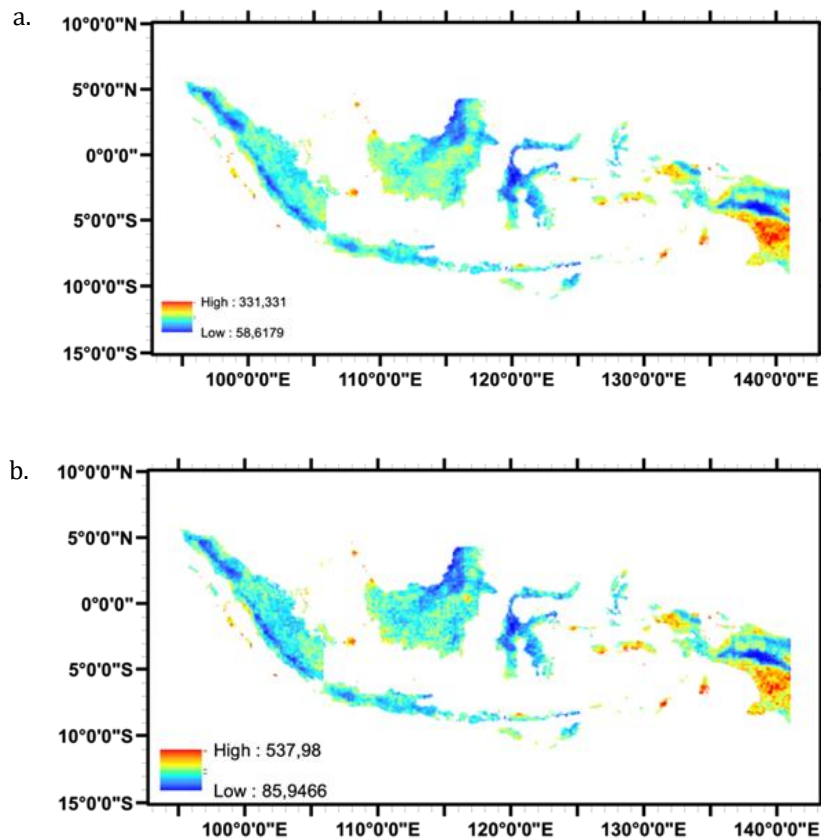


Fig. 6. (a) Rainfall for a 10-year recurrence period; (b) Rainfall for the 100-year anniversary period

3.2 Determination of GFI locations for sensitivity testing

In this study, the researcher selected regions with high extreme rainfall based on rainfall patterns to assess the sensitivity of the GFI method. The selected regions are presented in Table 1.

Table 1. Taking areas with extreme high rainfall based on rainfall patterns with a 100-year recurrence period

CH Pattern	Area	Rainfall (mm/day)	Level
Equatorial	Sumatera	287.49	medium
Local	Papua	314.41	high
Monsoonal	NTT	294.30	medium
Local	Maluku	323.91	high
Equatorial	Kalimantan	259.49	low
Monsoonal	Jawa	188.11	low

In Table 1, it can be observed that the average extreme rainfall for the 100-year return period is highest in local regions, with an average value of 323.91 mm/day in Maluku and 314.41 mm/day in Papua. Furthermore, regions with lower average extreme rainfall are Kalimantan and Java, with values of 259.49 mm/day and 188.11 mm/day, respectively.

3.3 Precipitation index a and b (lp-a and lp-b)

Bankfull discharge refers to a channel filled to its capacity without causing flooding. This condition is considered valid when the river remains in its natural state. Several researchers have investigated bankfull discharge in relation to return periods, including 1–2 years, 1–5 years, and less than 2 years. The determination of bankfull discharge is highly complex and depends on the classification of the river system. Therefore, in this study, a 5-year return period is used as the minimum threshold for non-flood conditions, assuming

that the river remains in its natural state. According to Aprianda (2022), the average extreme rainfall value for the 5-year return period at 120 BMKG observation stations was 146.78 mm/day and 143.56 mm/day, which closely aligns with BMKG's definition of extreme rainfall exceeding 150 mm/day.

In GFI processing, the flow accumulation in the modified GFI method is calculated using V_r . However, this cannot be applied if V_r values are not normalized, as the maximum value of flow accumulation per pixel is one. Therefore, rainfall normalization is required as an input parameter in the GFI calculation, using the proposed formula in Equation 4. It has been found that using I_p -A for the normalization of the 5-year return period results in an index value of zero; hence, the 5-year return period normalization is excluded from the GFI calculation as it is considered a non-flood condition.

The next proposed formula utilizes I_p -B, which is designed to assess flood variation based on extreme rainfall differences. This method introduces a slight modification to the upper threshold of the flood return period (P100) by using the average extreme rainfall value across Indonesia, as formulated in Equation 5. In regions with low extreme rainfall, the flood-prone area calculated using I_p -A is larger than that of I_p -B. Conversely, in regions with high extreme rainfall, the flood-prone area calculated using I_p -A is smaller than that of I_p -B.

3.4 GFI sensitivity testing

In this study, GFI sensitivity testing was conducted using both the conventional and modified methods, incorporating extreme rainfall at return periods of 10, 25, 50, and 100 years. Two methods were used: I_p -A and I_p -B. The results of the flood-prone area extent (hectares) are presented in Table 2.

Table 2. The size of the potential flood in Ha in each re-period using the a) I_p -A and b) I_p -B methods

I_p -A	P10	P25	P50	P100
Sumatera	19,962.5	28,650	32,506.25	35,962.5
Kalimantan	85,275	149,375	208,000	232,156.25
Papua	19,512.5	17,943.75	19,512.5	21,637.5
Java	14,837.5	24,656.25	29,837.5	35,512.5
East Nusa Tenggara (NTT)	8,087.5	10,900	12,150	13,831.25
Maluku	24,243.75	33,643.75	40,206.25	45,912.5
I_p -B	P10	P25	P50	P100
Sumatera	27,906.25	37,881.25	41,968.75	45,318.75
Kalimantan	151,168.75	234,012.5	275,043.75	303,675
Papua	29,806.25	38,975	45,556.25	48,343.75
Java	11,243.75	18,106.25	23,031.25	29,625
East Nusa Tenggara (NTT)	11,675	17,781.25	21,487.5	24,762.5
Maluku	56,118.75	82,293.75	96,050	107,287.5

In Table 2, it can be observed that the flood-prone area estimated using GFI I_p -A at a 100-year return period is equivalent to the conventional GFI. This is because the maximum GFI I_p -A index value is one. The extent of flood-prone areas in each region also significantly influences the total area assessed. As shown in section (c), Kalimantan has the largest flood-prone area, covering 232,156.25 hectares, while East Nusa Tenggara (NTT) has the smallest flood-prone area, covering 13,821.25 hectares.

Some regions exhibit larger flood-prone areas compared to section (a). The largest flood-prone area is in Kalimantan, reaching 303,675 hectares, whereas the smallest is in NTT, with 24,762.5 hectares. Additionally, certain regions show a larger flood extent using I_p -A compared to I_p -B, particularly in Java, with an area of 29,625 hectares. This occurs because Java has the lowest extreme rainfall among the sampled regions. To provide a clearer comparison between GFI I_p -A, I_p -B, and the conventional GFI, the data is presented in a graph shown in Figure 7 below.

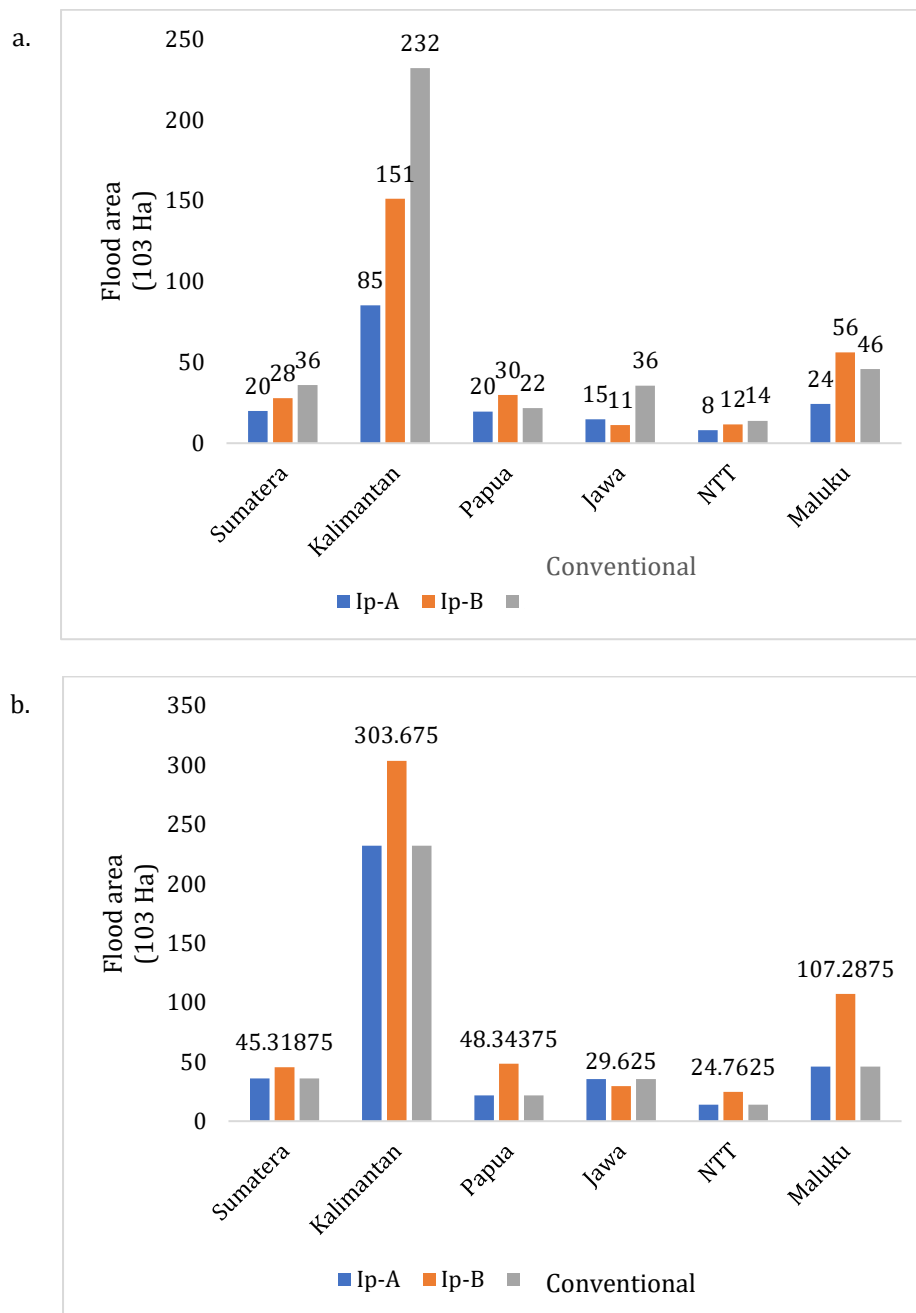


Fig. 7. (a) Graph of the area of potential flood area based on the 10-year recurrence period; (b) Graph of flood potential area based on 100-year recurrence period

Figure 7 is used to compare the flood-prone area in each region based on the specified return periods. The x-axis represents the sampled regions, along with GFI Ip-A (blue), Ip-B (orange), and the conventional GFI (gray), while the y-axis represents the potential flood area in each sample. The figure shows that as the return period increases, the flood-prone area also expands. In section (d), it is evident that the flood potential area for GFI Ip-A is identical to that of the conventional GFI.

In section (d), certain regions exhibit significant differences between GFI Ip-A and Ip-B. The graph for Jawa indicates that the flood-prone area estimated using Ip-B is smaller than that estimated using Ip-A. This occurs because Jawa has the lowest average extreme rainfall among the sampled regions. Conversely, in Maluku, the flood-prone area using Ip-B is larger than that using Ip-A, as Maluku has the highest average extreme rainfall among the sampled regions. Therefore, it can be concluded that the larger the average extreme rainfall in a region, the greater the estimated flood-prone area.

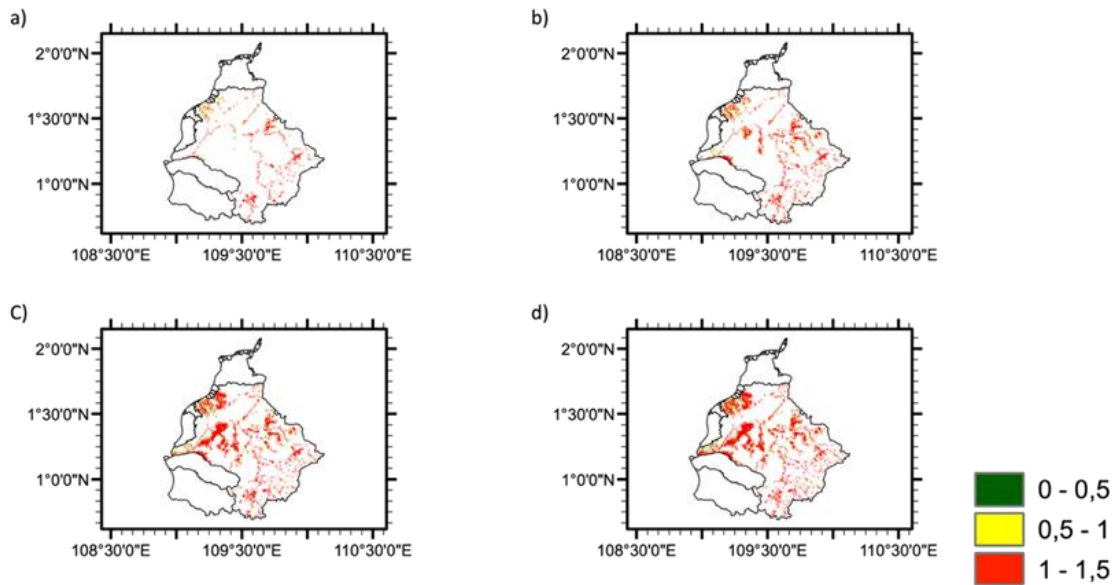


Fig. 8. (a) Potential flood area in the sample region (Kalimantan) using the Ip-A method with a 10-year return period; (b) Potential flood area in the sample region (Kalimantan) using the Ip-A method with a 25-year return period; (c) Potential flood area in the sample region (Kalimantan) using the Ip-A method with a 50-year return period; (d) Potential flood area in the sample region (Kalimantan) using the Ip-A method with a 100-year return period.

Figure 8 above presents the differences between GFI Ip-A and GFI Ip-B for one of the sampled regions, Kalimantan. Figure 8 illustrates the potential flood area for each return period using the Ip-A method. As the flood hazard level increases, the color intensity shifts towards red, whereas lower flood hazard levels are represented by green. The figure shows that red dominates the region, indicating a high flood hazard level in Kalimantan, primarily caused by extreme rainfall.

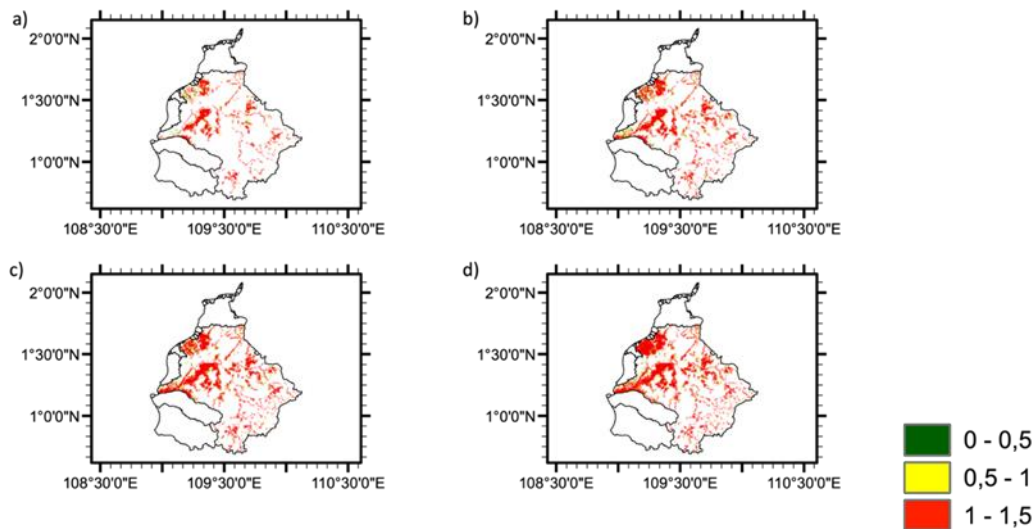


Fig. 9. (a) Potential flood area in the sample region (Kalimantan) using the Ip-B method with a 10-year return period; (b) Potential flood area in the sample region (Kalimantan) using the Ip-B method with a 25-year return period; (c) Potential flood area in the sample region (Kalimantan) using the Ip-B method with a 50-year return period; (d) Potential flood area in the sample region (Kalimantan) using the Ip-B method with a 100-year return period

Next, Figure 9 below illustrates the potential flood area using the Ip-B method for each return period. Similar to Figure 8, the flood hazard level increases as the color shifts towards red, while lower hazard levels are represented by green. The figure shows that red

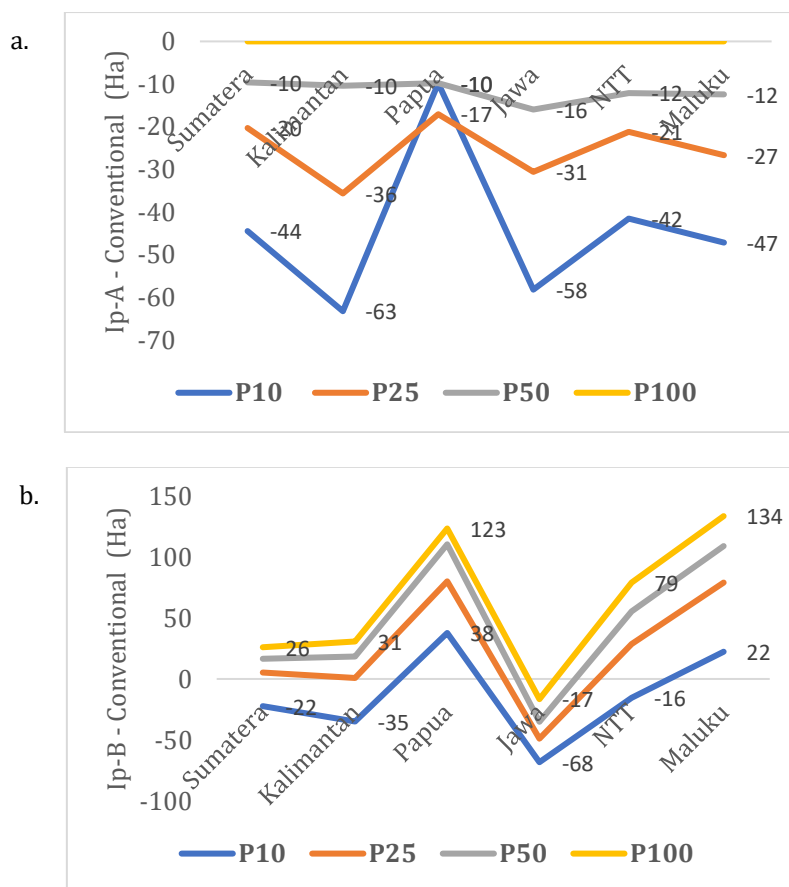
dominates the region, indicating a high flood hazard level in Kalimantan due to extreme rainfall. However, there are notable differences in flood extent across return periods compared to Figure 8. The red areas in Figure 9 are larger than those in Figure 8, demonstrating that the GFI Ip-B method is more sensitive to extreme rainfall, as the flood-prone area in Figure 9 is larger than in Figure 8.

3.5 Comparison of GFI hazard extent

The comparative analysis of the flood hazard extent between GFI Ip-A and Ip-B is conducted to highlight the differences in flood-prone areas between the two methods, which will be presented in Figure 10.

Section (a) explains the difference in flood extent between GFI Ip-A and the conventional GFI across different return periods. It is observed that as the return period increases, the flood-prone area estimated by GFI Ip-A gradually approaches that of the conventional GFI at the 100-year return period. This occurs because the maximum range of Ip-A is limited to 1, meaning that at the 100-year return period, GFI Ip-A becomes identical to the conventional GFI.

Section (b) illustrates the difference in flood extent between GFI Ip-B and the conventional GFI across return periods. The results show that as the return period increases, the difference in flood extent also grows. Some regions, such as Papua and Maluku, exceed the conventional GFI threshold as early as the 10-year return period, as these regions have the highest average extreme rainfall compared to other locations. This is followed by Kalimantan, Sumatra, and East Nusa Tenggara (NTT), which begin exceeding the conventional GFI threshold from the 25-year return period onward. Unlike the others, Java does not surpass the conventional GFI threshold even at the 100-year return period. This is due to Java's relatively low average extreme rainfall, which results in smaller flood-prone areas compared to the conventional GFI.



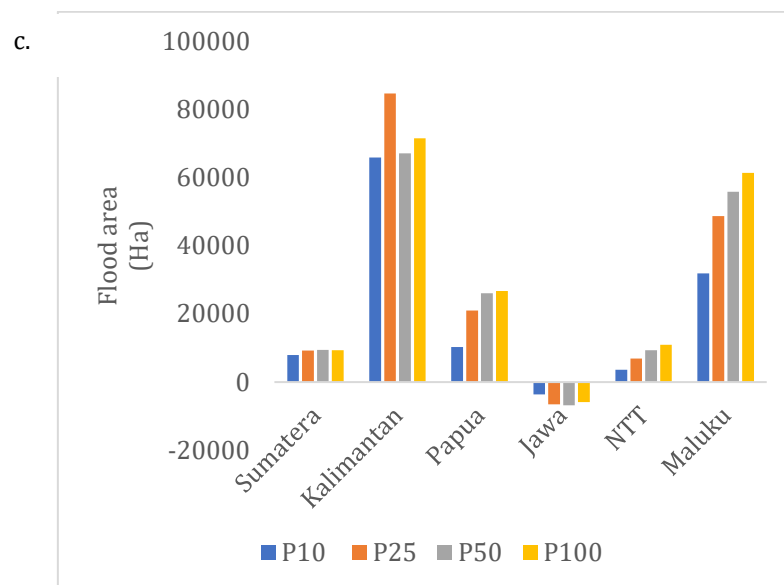


Fig. 10. (a) Different Ip-A flood areas compared to conventional GFI; (b) Different Ip-B flood areas compared to conventional GFI; (c) Ip-B – Ip-A

Section (c) presents the difference in flood extent between GFI Ip-B and GFI Ip-A across return periods. The graph is generated by subtracting the flood-prone area of GFI Ip-A from GFI Ip-B. The results show that Jawa is the only region in the sample where the flood-prone area estimated by Ip-B is smaller than that of Ip-A, with a difference of 5,887.5 hectares. This is due to Jawa having the lowest extreme rainfall among the sampled regions. Meanwhile, the largest flood extent difference is observed in Kalimantan, with an area of 71,518.75 hectares, as Kalimantan has both significant extreme rainfall and a vast land area.

3.6 Modified GFI in Indonesia

The results of the modified GFI using the Ip-A and Ip-B methods are presented in Figure 11 below. Figure 11 above illustrates the potential flood extent across Indonesia at the 100-year return period. In section (a), the flood-prone area in Belitung is not visible, whereas in section (b), a small flood-prone area can be observed. This occurs because Belitung experiences extreme rainfall, which becomes more evident when using the GFI Ip-B method. Therefore, it can be concluded that the greater the extreme rainfall, the more pronounced and extensive the potential flood area becomes.

The image presents a spatial distribution map of Indonesia, illustrating the intensity of a certain variable using a color gradient ranging from green to red. The green areas represent low intensity values between 0 and 0.5, yellow indicates moderate values from 0.5 to 1, and red highlights the highest intensity range, from 1 to 1.5. The map reveals that regions with dense concentrations of red, such as parts of Jawa, southern Sumatera, central Kalimantan, southern Sulawesi, and much of Papua, experience high levels of the mapped variable. In contrast, areas shown in green or lacking color likely have lower intensity or insufficient data coverage, which tends to be the case in more remote or less populated regions.

This spatial pattern suggests that the phenomenon being mapped—possibly population pressure, vulnerability, disaster risk, or a specific socio-economic indicator—is more intense in areas with higher human activity and settlement density. Such distribution is crucial for guiding development planning, resource allocation, or risk mitigation policies, as it highlights regions that may require more focused attention due to their higher intensity levels.

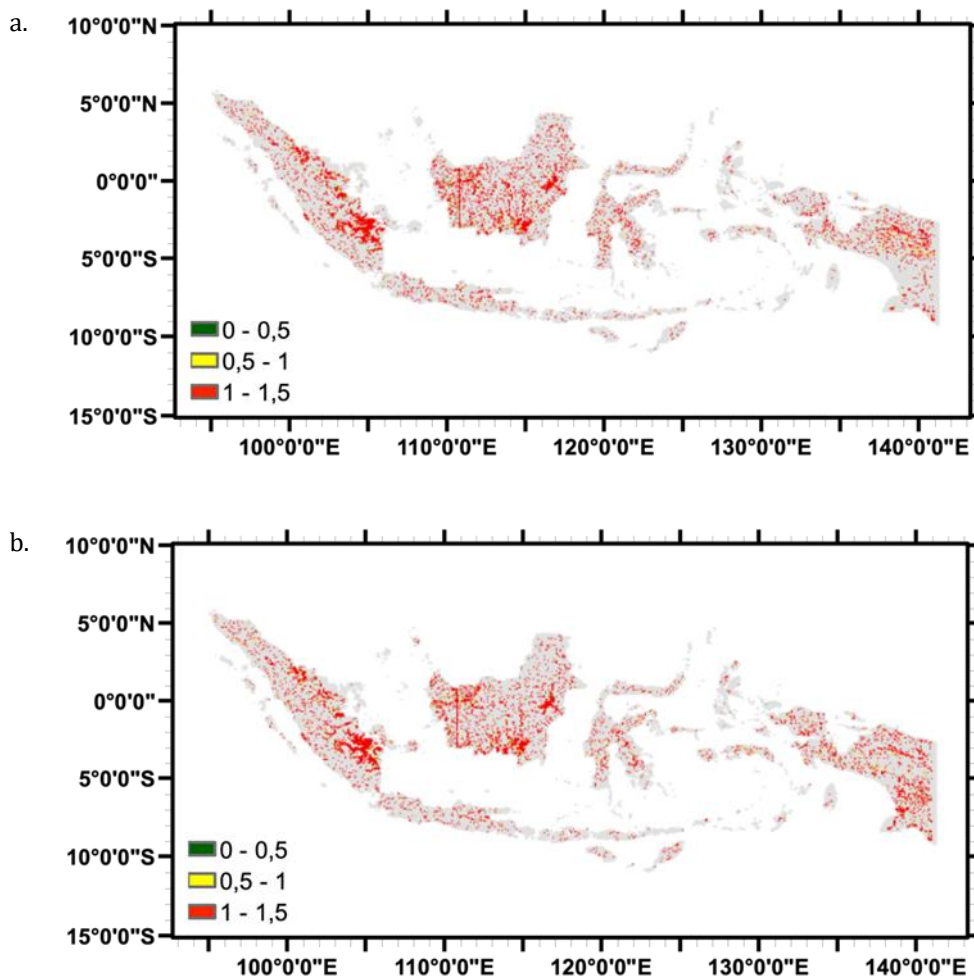


Fig. 11. (a) Comparison of potential flood areas throughout Indonesia using GFI Ip-A; (b) Comparison of potential flood areas throughout Indonesia using GFI Ip-B

4. Conclusions

When using the GFI Ip-A method at a 100-year return period, the potential flood area in Maluku is 35,512.5 hectares, while in Java, it is 45,912.5 hectares, and the GFI Ip-A method produces the same flood extent as the conventional GFI at this return period. Meanwhile, when using the GFI Ip-B method at a 100-year return period, Maluku has the highest extreme rainfall among the samples, with an average of 323.91 mm/day and a resulting flood-prone area of 107,287.5 hectares, whereas Java has the lowest extreme rainfall, with an average of 188.11 mm/day and a flood-prone area of 29,625 hectares, meaning that the GFI Ip-B method produces a different flood extent compared to the conventional GFI. Furthermore, the GFI Ip-B method shows that flood-prone areas correspond to the magnitude of extreme rainfall, indicating that the GFI Ip-B method is highly sensitive to extreme rainfall variations.

The recommendations that the author can provide are using better elevation data, such as SRTM, with the expectation that there will be no missing data, allowing for a more accurate estimation of flood-prone areas. Additionally, incorporating other parameters, such as land use, when applying the modified GFI method, to enhance the analysis. Furthermore, conducting tests with other indices, with the expectation of achieving more accurate results.

Acknowledgement

Author would like to express my sincere gratitude to the editorial team and reviewers for their invaluable contributions to this work. The author also acknowledges those who

provided assistance in language editing, proofreading, and technical writing, which greatly enhanced the quality of this manuscript.

Author Contribution

The author is solely responsible for the entire process of this research and article preparation. The contributions include formulating the research idea, data collection, data analysis, interpretation of the results, writing the manuscript, and final revisions prior to publication.

Funding

This research received no external funding.

Ethical Review Board Statement

Not available.

Informed Consent Statement

Not available.

Data Availability Statement

Not available.

Conflicts of Interest

The author declare no conflict of interest.

Open Access

©2024. The author. This article is licensed under a Creative Commons Attribution 4.0 International License, which permits use, sharing, adaptation, distribution and reproduction in any medium or format, as long as you give appropriate credit to the original author(s) and the source, provide a link to the Creative Commons license, and indicate if changes were made. The images or other third-party material in this article are included in the article's Creative Commons license, unless indicated otherwise in a credit line to the material. If material is not included in the article's Creative Commons license and your intended use is not permitted by statutory regulation or exceeds the permitted use, you will need to obtain permission directly from the copyright holder. To view a copy of this license, visit: <http://creativecommons.org/licenses/by/4.0/>

References

- Amri, M. R., Yuanti, G., Yunus, R., Wiguna, S., Adi, A. W., Ichwana, A. N., Randongkir, R. E., & Septian, R. T. (2016). *Risiko bencana Indonesia*. BNPB. [https://inarisk.bnpb.go.id/pdf/Buku%20RBI Final low.pdf](https://inarisk.bnpb.go.id/pdf/Buku%20RBI%20Final%20low.pdf)
- Aprianda, T. (2022). *Analisis Ambang Batas Nilai Curah Hujan Ekstrem di Indonesia*. Institut Teknologi Bandung.
- Barrocu, G., & Eslamian, S. (2022). Geomorphology and flooding. In *Flood Handbook* (pp. 23-54). CRC Press.
- Bastola, H., & Diplas, P. (2023). Modeling bankfull channel geometry based on watershed and precipitation characteristics using dimensionless parameters. *Water Resources Research*, 59(6), e2022WR032688. <https://doi.org/10.1029/2022WR032688>
- Bellos, V. (2012). Ways for flood hazard mapping in urbanised environments: A short. *Water Util. J*, 4, 25-31. https://www.ewra.net/wuj/pdf/WUJ_2012_04_03.pdf
- Fisher, R. A., & Tippett, L. H. C. (1928). *Limiting Forms of the Frequency Distribution of the Largest or Smallest Members of a Sample*. Proceedings of the Cambridge Philosophical Society, 24, 180-190. <http://dx.doi.org/10.1017/S0305004100015681>
- Ghafuri, B., Montazeri, A., & Eslamian, S. (2024). *Bankfull Stage and Discharge: A*

- Comprehensive Review*. Handbook of Climate Change Impacts on River Basin Management, 328-336.
- Haan, N. (1977). A Tripartite Model of Ego Functioning: Values and Clinical Research Applications. *The Journal of Nervous Mental Disorders*, 148, 14-30. <https://doi.org/10.1097/00005053-196901000-00003>
- Hafiz, A., Nugraha, A., Ichwana, A. N., Nugroho, P., Septian, R. T., Randongkir, R. E., Pinuji, S. E., & Syauqi. (2019). Petunjuk Teknis Penyusunan Kajian Risiko Bencana Banjir. BNPB. https://coastalresilience.bnpb.go.id/wp-content/uploads/2024/04/MODUL-TEKNIS_KRB_GEA.pdf
- Kubro, S. (2021). *Modifikasi Metode Geomorphology Flood Index Menggunakan Parameter Curah Hujan*. Institut Teknologi Bandung.
- Manfreda, S., & Samela, C. (2019). A digital elevation model based method for a rapid estimation of flood inundation depth. *Journal of Flood Risk Management*, 12(1), e12541. <https://doi.org/10.1111/jfr3.12541>
- Manfreda, S., Samela, C., Gioia, A., Consoli, G. G., Iacobellis, V., Giuzio, L., ... & Sole, A. (2015). Flood-prone areas assessment using linear binary classifiers based on flood maps obtained from 1D and 2D hydraulic models. *Natural Hazards*, 79, 735-754. <https://doi.org/10.1007/s11069-015-1869-5>
- Mudashiru, R. B., Sabtu, N., & Abustan, I. (2021). Quantitative and semi-quantitative methods in flood hazard/susceptibility mapping: a review. *Arabian Journal of Geosciences*, 14(11), 941. <https://doi.org/10.1007/s12517-021-07263-4>
- Parker, T., & Gallant, A. J. (2022). The role of heavy rainfall in drought in Australia. *Weather and Climate Extremes*, 38, 100528. <https://doi.org/10.1016/j.wace.2022.100528>
- Qiao, S., Zeng, G., Wang, X., Dai, C., Sheng, M., Chen, Q., ... & Xu, H. (2021). Multiple heavy metals immobilization based on microbially induced carbonate precipitation by ureolytic bacteria and the precipitation patterns exploration. *Chemosphere*, 274, 129661. <https://doi.org/10.1016/j.chemosphere.2021.129661>
- Rosgen, D. L. (1994). A classification of natural rivers. *Catena*, 22(3), 169-199. [https://doi.org/10.1016/0341-8162\(94\)90001-9](https://doi.org/10.1016/0341-8162(94)90001-9)
- Samela, C., Albano, R., Sole, A., & Manfreda, S. (2018). A GIS tool for cost-effective delineation of flood-prone areas. *Computers, Environment and Urban Systems*, 70, 43-52. <https://doi.org/10.1016/j.compenvurbsys.2018.01.013>
- Samela, C., Troy, T. J., & Manfreda, S. (2017). Geomorphic classifiers for flood-prone areas delineation for data-scarce environments. *Advances in water resources*, 102, 13-28. <https://doi.org/10.1016/j.advwatres.2017.01.007>
- Sarker, S. (2023). Separation of floodplain flow and bankfull discharge: application of 1D momentum equation solver and MIKE 21C. *CivilEng*, 4(3), 933-948. <https://doi.org/10.3390/civileng4030050>
- Sherwood, J. M., & Huitger, C. A. (2005). *Bankfull Characteristics of Ohio Streams and Their Relation to Peak Streamflows*. U.S. Geological Survey Scientific Investigation Report 2005-5153. https://pubs.usgs.gov/sir/2005/5153/pdf/Bankfull_book.pdf
- Shojinaga, R., Hamilton, D., Burford, M. A., & Sobota, D. J. (2025). The effects of climate and geomorphology on bankfull conditions in subtropical Australian streams. *Journal of Hydrology: Regional Studies*, 59, 102356. <https://doi.org/10.1016/j.ejrh.2025.102356>
- Suryadi, Y. (2007). *Metoda Penentuan Indeks Banjir Berdasarkan Fungsi Debit Puncak Hidrograf Inflow, Luas Genangan, Kedalaman Genangan, dan Waktu Genangan (Studi Kasus pada DAS Citarum Hulu)*. Institut Teknologi Bandung.
- Teng, J., Jakeman, A. J., Vaze, J., Croke, B. F., Dutta, D., & Kim, S. J. E. M. (2017). Flood inundation modelling: A review of methods, recent advances and uncertainty analysis. *Environmental modelling & software*, 90, 201-216. <https://doi.org/10.1016/j.envsoft.2017.01.006>
- Van Campenhout, J., Houbrechts, G., Peeters, A., & Petit, F. (2020). Return period of characteristic discharges from the comparison between partial duration and annual series, application to the Walloon Rivers (Belgium). *Water*, 12(3), 792. <https://doi.org/10.3390/w12030792>

- Wu, B., Wang, G., Xia, J., Fu, X., & Zhang, Y. (2008). Response of bankfull discharge to discharge and sediment load in the Lower Yellow River. *Geomorphology*, 100(3-4), 366-376. <https://doi.org/10.1016/j.geomorph.2008.01.007>
- Zarrabi, R., McDermott, R., Erfani, S. M. H., & Cohen, S. (2025). Bankfull and Mean-Flow Channel Geometry Estimation Through Machine Learning Algorithms Across the CONTiguous United States (CONUS). *Water Resources Research*, 61(2), e2024WR037997. <https://doi.org/10.1029/2024WR037997>
- Zin, W. W., Kawasaki, A., Takeuchi, W., San, Z. M. L. T., Htun, K. Z., Aye, T. H., & Win, S. (2018). Flood hazard assessment of Bago river basin, Myanmar. *Journal of Disaster Research*, 13(1), 14-21. <https://doi.org/10.20965/jdr.2018.p0014>

Biographies of Author

Jessica Amanda Bintang, Study Program of Meteorology, Faculty of Earth Sciences and Technology, Institut Teknologi Bandung, Bandung, West Java 40132, Indonesia.

- Email: jessicaamnd@gmail.com
- ORCID: N/A
- Web of Science ResearcherID: N/A
- Scopus Author ID: N/A
- Homepage: N/A